MODELLING HUMAN GAIT USING A NONLINEAR DIFFERENTIAL EQUATION

Jelena Schmalz[a], David Paul[a], Kathleen Shorter[a], Xenia Schmalz[b], Matthew Cooper[a], Aron Murphy[c]

[a]University of New England, School of Science and Technology, Armidale, NSW, Australia

[b]Department of Child and Adolescent Psychiatry, Psychosomatics and Psychotherapy, University Hospital, LMU, Munich, Germany

[c]Faculty of Medicine, Nursing and Midwifery and Health Sciences, University of Notre Dame, Australia

Abstract We introduce an innovative method for the investigation of human gait, which is based on the visualisation of the vertical component of the movement of the centre of mass during walking or running, in the space of the coordinates position, velocity, and acceleration of the centre of mass. We collected data and numerically approximated the gait by the best-fitting curve for a non-linear model. The resulting equation for the best fitting plane or curve in this space is a differential equation of second order. The model that we suggest is a Duffing equation with coefficients that depend on the height of a walker or runner and on the angular frequency of the oscillation. We present statistical analyses of the distribution of the Duffing stiffness depending on the speed.

Keywords: dynamical systems, Duffing equations, non-linear differential equations, biomechanics, biodynamics, gait modelling

1. INTRODUCTION

Research on the mechanics of human gait is of interest to different disciplines, for example sport science, medicine, and robotics. In this paper, we introduce a model for the movement of the vertical coordinate of a person's centre of mass (COM) during walking and running.

Human locomotion is an inherently complicated process requiring the complex integration of neural control and musculoskeletal dynamics in response to both internal and external forces. In an attempt to strip away complexity and gain an understanding of the fundamental principles underpinning human locomotion, simple mechanical models have been developed [1, 2]. The mechanical simplification of locomotion allows the identification of just a few key parameters that can be manipulated to examine cause and effect relationships and identify which features most influence the system.

Blickhan suggested a linear spring-mass model for hopping in 1989, [3]. Other papers followed, for example [4–7]. The motion of the centre of mass is described by the equation $mz_{tt} + Kz = -mg$, where m is the body mass, z is the vertical deflection of the centre of mass with the origin on the treadmill surface and the direction chosen upwards. The constant K is the stiffness, and g is gravitational acceleration. By z_{tt} we denote the second derivative of z, i.e., the vertical acceleration of the centre of mass. There have been different approaches on how to calculate leg stiffness. Blickhan's approach uses the formula $K = m\omega_0^2$, where ω_0 is the stride's angular frequency of the oscillation, which, during gait, reflects the stride's angular frequency. [3, 6]. Another approach for calculation of the leg stiffness is to find the ratio of F_m, the maximum value of the vertical ground reaction force, and ΔL, the absolute value of the leg compression, i.e., $K = \frac{F_m}{\Delta L}$. This definition of leg stiffness is used in several publications [4, 5, 7–9; see 6 for an overview]. There is a third approach to leg stiffness calculation based on the measurements of loss of mechanical energy by walking/running, W. Leg stiffness K is derived from the formula $W = \frac{1}{2}K(\Delta r)^2$, where Δr is the shortening of a spring (e.g. [10]). In examining mechanical and metabolic determinants of the human walking gait, Kuo [11, 12] employed an anthropomorphic three-dimensional, passive-dynamic model, in which human legs were represented as rigid inverted pendulums with small point masses modelling each foot and a larger mass modelling the concentration of the COM at the pelvis. These studies drew on earlier models of a rigid swing leg during walking [13] and continued the view that walking and running were two distinct gaits that could not be

described using similar mechanical models. This view, however, was discounted by Geyer, Seyfarth, Blickhan (2006) [14] who demonstrated that a compliant-legged, spring-mass bipedal model consisting of two linear, equal and massless springs and a single COM point as an extension of Blickhan's one-dimensional model, reliably predicted ground reaction forces and COM behaviour in both human walking and running. Several subsequent studies further validated the efficacy of a bipedal spring-mass model of walking [2, 15–18]. While much of the twenty-first century research in the field has adopted the bipedal spring-mass model and focused on adapting or adding selected elements to improve prediction accuracy for both walking and running gait mechanics, Blickhan's spring-mass model remains largely valid and has been applied, with modifications to suit certain parameters, in recent studies [19, 20].

Our mathematical model is based on the analysis of three-dimensional movement of COM. We concentrate on the projection of the movement of COM on the vertical axis. We suggest a new approach for finding leg stiffness for the simple harmonic oscillation model, and then develop a more precise model assuming that the stiffness for a fixed speed is not a constant but depends on the displacement of the COM. The innovative idea of our method is to visualise the data for the vertical component of a motion of the COM, $z(t)$, as a curve in the three-dimensional space, (z, z_t, z_{tt}) (see Section 2). Here z_t and z_{tt} are the first and the second derivatives of the function $z(t)$, velocity and acceleration, correspondingly. The linear differential equation $z_{tt} + \frac{K}{m}(z - z_0) = 0$, which is a simple harmonic oscillation model of a gait, can be interpreted as an equation of the plane in the space (z, z_t, z_{tt}). Here K is the leg stiffness, m is the mass of a participant, and z_0 is the average z-coordinate of the COM by the movement. Finding the best fitting plane to the data curve gives us the slope of the plane $\frac{K}{m}$ and the value of z_0. This simple model suggests that the leg stiffness is a constant. But we can observe that the slope in general is not a constant (see for example Fig.2), but can be represented as a non-linear model with a cubic term. Thus, we use a non-linear differential equation model, approximating the curves by the Duffing equation. The best fitting curves have the form $z_{tt} + kz(z - z_0)(h - z) = 0$. Here h is the height of a participant in motion. We called the value km Duffing stiffness. The constant k is different for each participant and increases with the speed of walking/running. We first analyse how Duffing stiffness relates to speed using data for six participants collected by us, then verify the results using data publicly available for 42 walking participants and 29 running participants [21, 22].

Modelling of gait by Duffing equations emphasises the commonalities of stable walking and running. However, the curves also contain individual features for each person and velocity. We provide examples of the variety of these curves in Section 8. Studying outliers might be more interesting for sport science, because they are a sign of some anomalies and instability in gait, which might, for example, suggest an injury.

2. DATA RECORDING

We collected walking and running data from six participants (aged 18 to 55 years, 3 men and 3 women). The study followed ethical protocols as per ethics requirements (HE19- 239). We measured the vertical coordinates $z(t)$ of the COM for each participant walking or running on the treadmill. The markers were the Left and Right PSIS and ASIS; we then computed the average of all four. The data was collected for different integer velocities, at 100 frames per second, over 10 seconds, for each velocity, using an 8 camera, Qualisys Motion capture system with the COM reconstructed using a pelvic marker set within Visual3D.

Using MATLAB, we visualised the data as curves in the three-dimensional space (z, z_t, z_{tt}). We filtered out high frequency oscillations, such as noise and individual features, using the fast Fourier transform function in MATLAB. The direction of the motion along the curve can be found, for example, in the following way. Find the point with the greatest z-coordinate. This is the highest point of the centre of mass during the gait cycle. The velocity at this point is equal to zero. Hereafter, the movement goes down, i.e., the velocity z_t becomes negative. In both pictures of Figure 1, from those perspectives, the movement is clockwise.

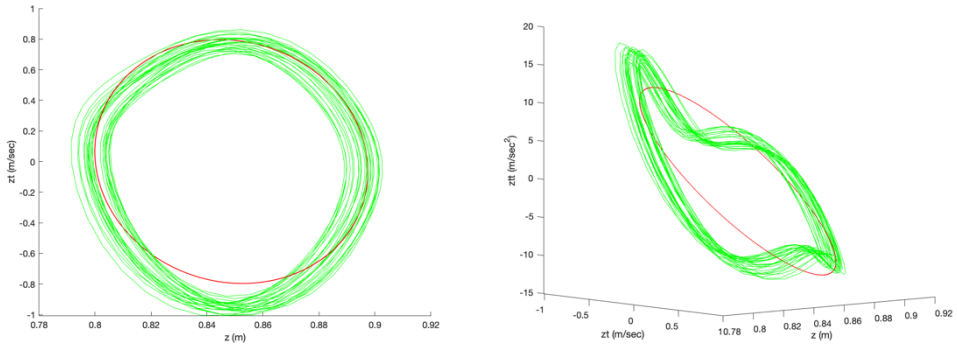

Fig 1. A MATLAB 3D figure shown from different perspectives. The green curve is a smoothed data curve with high-pass FFT threshold 0.03, the red curve is a smoothed data with FFT threshold 0.3.

3. DATA INTERPRETATION

The pictures in the space with the coordinates position, velocity, and acceleration, are rich in information. For example, Figures 2 and 3 show the data for walking (4 km/hr) and running (9 km/hr), respectively, of the same participant.

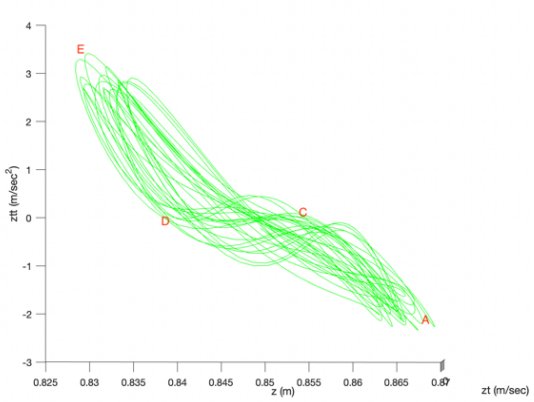

Fig 2

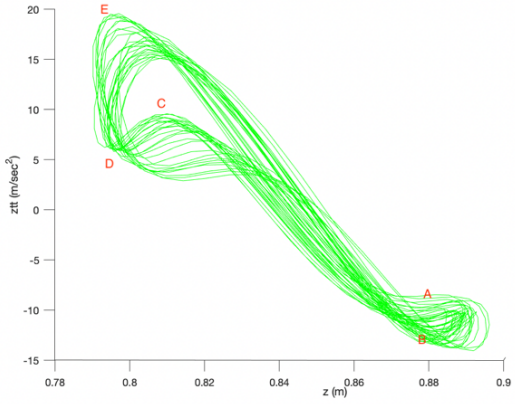

Fig 3

Figs 2 and 3 show data for walking, 4 km/hr and for running, 9 km/hr, correspondingly. The horizontal axis shows position and the vertical axis the acceleration of the COM. In both Figs, the part CD corresponds to the phase of the gait when a foot touches the surface, DE corresponds to the propulsion during toe-off, during EA the COM moves upwards and the acceleration diminishes. The arc AB appears only in Fig 3 and corresponds to the flight phase

Here we look into the projection to the plane z, z_{tt}, i.e., the horizontal axis shows the position of the COM (in meters) and the vertical axis shows the acceleration (in m/sec^2). The part CD of both curves corresponds to the phase of the gait when a foot touches the surface of the treadmill. In the case of walking, it is a flat line; vertical acceleration is close to zero. In the case of running, acceleration is diminishing because of braking during initial foot contact. The phase DE corresponds to the propulsion during toe-off, where acceleration (and consequently force) increases. On the segment EA acceleration diminishes, turns to zero when the COM reaches its average position, and is minimal at the point A. The minimum acceleration for the walking curve is -2 m/sec^2, the minimum acceleration for the running curve is about -10 m/sec^2, i.e., close to the gravitation constant g. The acceleration is less during walking than during running because the body is always in contact with the ground whereas during running there is a flight phase.

The arc AB on Figure 3 corresponds to the flight phase of running. This part of the curve is more complicated than just a flat constant $z_{tt} = -g$, because it is smoothly connected with the rest of the curve. Some information that we get from these curves is common for all participants and walking/running speeds, but some features are individual – for example not each participant has the "flight" component AB at running speeds, due to individualised transitions between walking and running gait patterns. In this paper we concentrate on their common properties, and suggest three models, based on differential equations. We build our three models based on data, purely numerically and mathematically.

4. MODELLING GAIT AS HARMONIC OSCILLATOR

By Hook's Law [23], a movement of a spring with stiffness K satisfies the equation

(1) $mz_{tt} + K(z - z_0) = 0,$

where m is the mass, K is stiffness and $z - z_0$ is the displacement of the COM. In three-dimensional space (z, z_t, z_{tt}), Eq (1) is the equation of a plane that passes through the point $(z_0, 0, 0)$. We find the coefficients in Eq. (1) numerically, by finding the best fitting plane for the smoothed data curve. The initial values specify the ellipse on this plane. The gravitation constant is included in Eq. (1) implicitly. We can rewrite the equation as

(2) $mz_{tt} + K(z - z_{st}) = -mg.$

The coordinate z_{st} is the average of the vertical coordinate of the centre of mass of a standing body but in a walking/running posture. It is not exactly the same as the coordinate of COM in a standing position. The relation between z_0 and z_{st} is calculated from Eqs. (1) and (2) and is $z_0 = z_{st} - \frac{mg}{K}$.

5. MODELLING BY A NON-LINEAR HOMOGENEOUS DIFFERENTIAL EQUATION

5.1. Best fitting curve, interpreted as a non-linear second order differential equation. Non-linear gait dynamics has been discussed, for example, in [24]. Stride-to-stride fluctuations, which are often considered to be noise, actually convey important information. To describe these fluctuations, we refine the method used for the harmonic oscillation model in section 4. We approximate the movement of the COM during walking or running by a Duffing equation, i.e., a homogeneous non-linear second order differential equation. We write

(3) $mz_{tt} + K(t)(z - z_0) = 0,$

where, unlike the harmonic oscillation model from Section 4, we consider stiffness to not be constant, but as dependent on time, $K(t)$, as stiffness and viscosity depend on a phase of a stride. For example, the slope on Figures 2 and 3 depends on $z(t)$, and the slope in the plane z, z_{tt} reflects stiffness: it is $\frac{K(t)}{m}$ at a time t. We divide both sides by m and consider the approximation of the function $k(t) = \frac{K(t)}{m}$ by polynomial,

(4) $z_{tt} + (k_1(z - z_0) + k_2(z - z_0)^2 + k_3(z - z_0)^3) = 0.$

As the value z_0 is not known beforehand, we look for the best fitting curves of the form:

(5) $z_{tt} + k_1 z + k_2 z^2 + k_3 z^3 + C = 0.$

The best fitting curve in the chosen coordinates is a differential equation of second order. Initial conditions are the values $z(0)$ and $z_t(0)$. We visualize the solution of this differential equation as a curve in the same coordinate system as the data curve. See, for example, Figure 4, where the red curve is the data curve, and the blue curve is the solution of the differential equation given by the best fitting curve. We computed a scaled

mean squared error between the Duffing equation output and the observed data. As the values z, z_t and z_{tt} have different units, we scaled each value by dividing by the difference between the minimum and maximum values on the corresponding axis.

5.2. Finding and analysing the fixed points. We are also interested in the fixed (equilibrium) points [25]. We first rewrite the second order differential Eq. (5) as a system of first order differential equations:

(6) $z_t = z_1,\ (z_1)_t = -k_1 z - k_2 z^2 - k_3 z^3 - C.$

We found the fixed points by solving the equilibrium equations (see for example [26])

(7) $z_1 = 0,\ -k_1 z - k_2 z^2 - k_3 z^3 - C = 0.$

The solutions to Eq. (5) are plotted in the same coordinate system as the data curves, see for example Figure 4. The solution curves are stable if we set one fixed point equal to zero, i.e., $C = 0$. Then the two other fixed points occur at z_0 (the centre of the closed curve, average coordinate of the centre of mass during walking/running), and at h for stable walking/running. The differential equation Eq. (5) becomes

(8) $z_{tt} + kz(z - z_0)(h - z) = 0.$

Numerical computations show that, for stable gait, the fixed point $z = z_0$ is a centre, while the fixed points $z = 0$ and $z = h$ are saddles.

5.3. Interpretation of the parameters in the model. Eq. (8) shows that we can model the movement of COM with a Duffing equation, up to a constant k, knowing only h and z_0. The values h and z_0 are close to the height of a person and to the average coordinate of the COM in motion, correspondingly. The gravitation constant g is involved implicitly in the differential equation, in a similar way as in the harmonic oscillation model in Section 4. The coefficient k does not have the meaning of the square of the angular frequency, $\omega^2 = \frac{stiffness}{mass}$, as in a linear case (Section 4), but k behaves in a similar way: it increases with an increase of the walking/running speed. We call this constant, multiplied by the mass, the **Duffing stiffness**. The meaning of the coefficient k is found from the following consideration. We rewrite Eq. (8) as $z_{tt} + k[-(z - z_0)^3 + (h - 2z_0)(z - z_0)^2 + z_0(h - z_0)(z - z_0)] = 0$. For z close to z_0 the linear approximation at z_0 is

(9) $z_{tt} + kz_0(h - z_0)(z - z_0) = 0.$

Comparing this equation with Hook's Law (Eq. (1)) we get an expression that relates the angular frequency ω with the coefficient k and the values z_0 and h: $\omega^2 \approx kz_0(h - z_0)$. Hence, the Duffing stiffness

(10) $mk \approx \frac{m\omega^2}{z_0(h-z_0)} = \frac{K}{z_0(h-z_0)}.$

We used that leg stiffness K is expressed as $K = m\omega^2$. Assuming the model when the centre z_0 is approximately in the middle between two saddle points, 0 and h, we get $h = 2z_0$, and Eq. (15) becomes symmetrical,

(11) $z_{tt} + kz_0^2(z - z_0) - k(z - z_0)^3 = 0$, where $k > 0$,

and $k \approx \frac{\omega^2}{z_0^2}$. Eq. (11) is the Duffing equation for a softening oscillator [26], i.e., the stiffness diminishes with the displacement.

5.5. Example based on the collected data. Figure 4 shows the observed smoothed data curve (red) and the curve corresponding to the solution of Eq. (8) (blue) for one of the participants, together with the fixed points.

The differential equation that describes the movement of the centre of mass of this participant running at the speed 8 km/hr is $z_{tt} + 279(z - 0.9)(1.8 - z) = 0$. We have rounded k to an integer, and z_0 and h to the first decimal place. From $k = 279$, $z = \frac{1}{2}h = 0.9$ we can compute $\omega \approx \sqrt{\frac{k}{z_0^2}} \approx 18.56$, i.e., the number of strides in a second is $\frac{\omega}{2\pi} \approx 2.95$. This participant made 24 strides in 10 secs, i.e., the real number of strides in a second is 2.4.

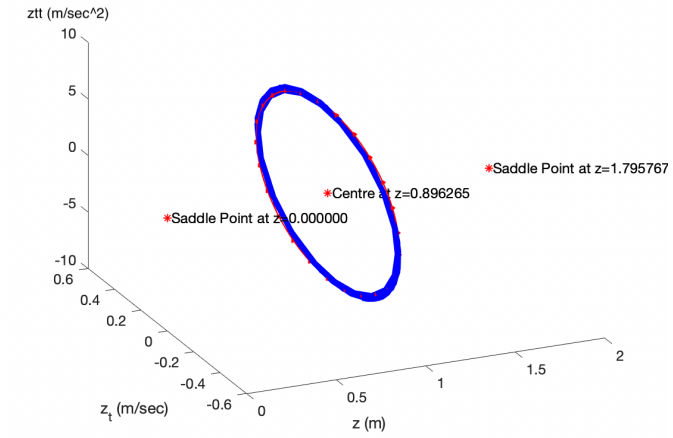

Fig 4. Curve (blue) for the solution to Eq. (8) for a participant (178cm tall, running at 8 km/h) compared with the data curve (red). The mean squared error is 0.015. The fixed points are saddles at $z = 0$ and $z \approx 1.8$ and the centre at $z_0 \approx 0.9$

6. STATISTICAL ANALYSIS

6.1. (University of New England (UNE) data. Fig.5 (left) shows that the Duffing stiffness depends on the speed of walking/running for each participant. By visually inspecting the graph, we see some outlier points. To further examine these, we calculated the standard deviation of Duffing stiffness for each participant, for the walking data. Two participants had standard deviations (SDs) > 400, while the rest of the participants had SDs < 100. Our observation of these two participants during the data recording showed that they were uncomfortable with some of the speeds, and they reported having no experience with treadmills. Therefore, we excluded these two participants from all further analyses. Fig.5 (right) shows the data for the remaining four participants.

The behaviour of the Duffing stiffness is different for walking (3 - 8 km/hr) and running (9 - 14 km/hr). Therefore, we separately fit data for walking and running speeds. We fitted a Linear Mixed Effect model in R for the walking data. We included speed as the fixed effect and Duffing stiffness as the dependent variable. We allowed both the slopes and the intercept to vary across participants. The model showed a slope estimate of $\hat{\beta}$=41.4, $t = 9.1$, $p = 0.004$. For the running data, we performed an equivalent analysis. Here, the slope associated with speed trended in a positive direction, $\hat{\beta} = 13.9$, $t = 3.0$, $p = 0.05$.

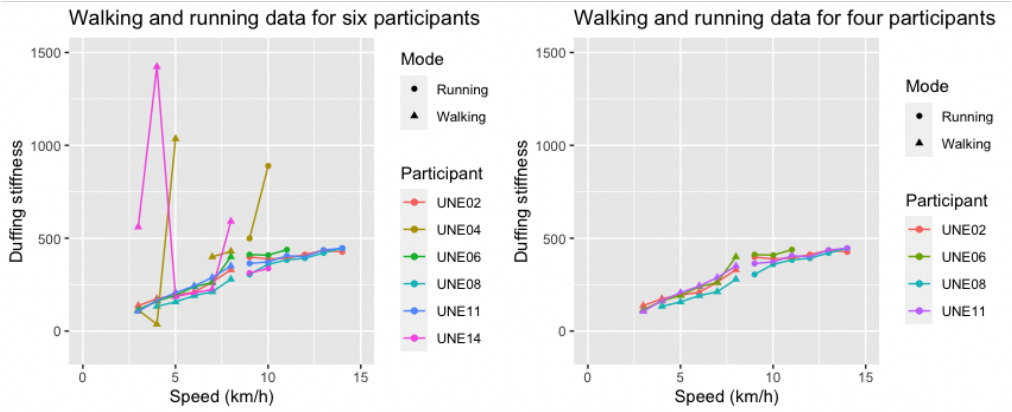

Fig 5. Duffing stiffness depending on speed with and without outliers. We consider the models for walking and for running separately. Each line represents a different participant

6.2. Comparing UNE dataset against public datasets. Next, we compare our data against public datasets for 42 walking participants [21], and 29 running participants [22]. As these sources were set up slightly differently than the UNE data, in order to match the data, we estimated the COM during walking or running, using the midpoint of the ASIS markers and subtracting the lowest value for the heel's marker.

Figure 6 shows the relationship between speed and Duffing stiffness.

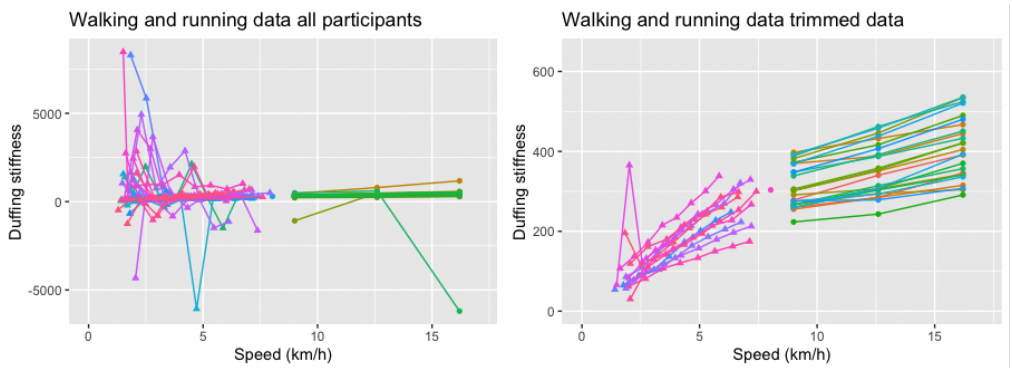

Fig 6. Duffing stiffness as a function of speed, with and without outliers. Note that the Duffing stiffness, k, depends also on the height of the COM of a participant, z_0, and the angular frequency of walking/running, ω: $k \approx \frac{\omega^2}{z_0^2}$.

First, we removed one participant with only one data point. Then, to identify outliers, we calculated the SDs in Duffing stiffness for each participant and excluded outliers for the walking and the running datasets, separately. For the walking data, [22], the SDs ranged from 39.2 to 3183.5. We chose to remove all participants with SD > 100. This left us with 12 participants for the walking data. We proceeded to fit the data with a Linear Mixed Effect model, akin to the UNE data. Again, we get a significant effect of speed on Duffing stiffness, $\hat{\beta}$=36.7, $t = 11.8$, $p < 0.0001$. For the running data, [21], we removed three out of 29 participants with SD > 100. The Linear Mixed Effect model showed a significant effect of speed, $\hat{\beta} = 13.5$, $t = 14.0$, $p < 0.0001$.

Finally, we compared the two datasets against each other. We created two models, one for running and one for walking, including both of the trimmed datasets. In the Linear Mixed Effect model, Duffing stiffness acted as the dependent variable, and the fixed effects were speed, dataset UNE versus [21, 22], with UNE acting as a baseline. We allowed the slope and the intercept to vary across participants. For walking, the effect of speed was, again, significant, $\hat{\beta} = 36.7$, $t = 12.4$, $p < 0.0001$. However, the effect of dataset was not significant, $\hat{\beta} = -43.1, t = -1.5, p = 0.2$, nor was the interaction between dataset and speed, $\hat{\beta} = 5.3,\ t = 0.9,\ p = 0.4$.

Similarly, in the running dataset, the effect of speed was $\hat{\beta} = 13.5,\ t = 13.2,\ p < 0.0001$. Neither the effect of dataset, nor the interaction of dataset and speed were significant, $\hat{\beta} = 27.5,\ t = 0.9,\ p = 0.4$ and $\hat{\beta} = 3.4,\ t = 1.1,\ p = 0.3$, respectively.

In summary, we found, overall, a significant positive relationship between speed and Duffing stiffness. For the running UNE data, the slope was not significant; however, when we combined the two datasets, the running slope was significant, and we found no interaction. Thus, the lack of significance in the UNE running data may be a result of low statistical power. We found no main effect of dataset, nor an interaction between dataset and speed. Thus, we find no evidence of a difference across datasets.

6.3. Identifying and examining outliers. From a practical perspective, an interesting aspect is participants whose data deviates from the fitted model. Here, we defined outliers based on SDs. This is the simplest method, which can easily be applied by a sport scientist without mathematical training. We drew a somewhat arbitrary threshold, where we treated all participants with a SD $>$ 100 as outliers. The reasons for high SD could vary across participants. For example, a typical problem for uncomfortable speeds less than 3 km/hr is an additional loop, as on the red line in Fig.7. The Duffing equation does not take into account the loop, as the blue approximation curve demonstrates. The other example of an outlier is illustrated in Fig. 8, where the curve breaks down into two parts, corresponding to the left or to the right leg. Red lines represent the data, blue lines are the solutions of the differential equation. A third reason for outliers that we noticed is an instability of walk, when each step varies in the amplitude and in the average height.

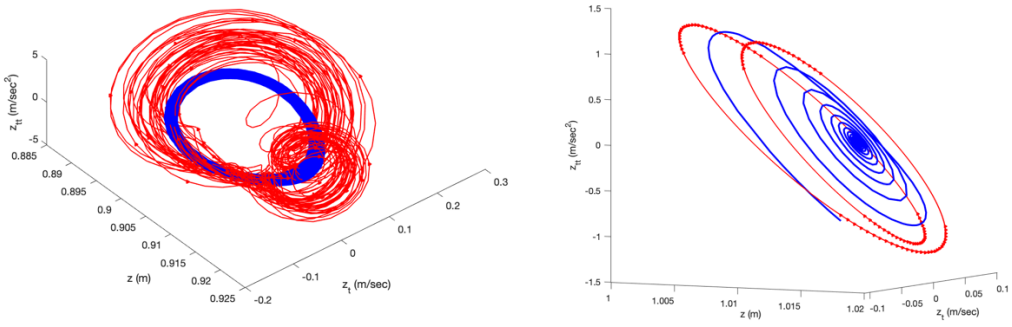

Fig 7. Slow walking speeds (< 3 km/hr, FTT=0.03) often contain an additional loop because of the compelled braking during each step

Fig 8. Asymmetry of the gait (4.7 km/hr) due to different strengths of the left and the right legs. The red curve brakes down into two parts, corresponding to the left or to the right leg

7. DUFFING EQUATION WITH VISCOSITY AND EXCITATION FORCE

7.1. Motivation. Approximation by a homogeneous equation with zero viscosity does not take into account the asymmetry caused by damping and excitation forces. For example, the red curve in Figure 9 shows a smoothed data curve for a running participant (14 km/hr, FFT threshold=0.3) in the phase plane (z, z_t). This curve is close to an ellipse, and the absolute value of the slope of the main axis of the ellipse, AC, is equal to $v = \frac{\nu}{m}$ if we assume that the viscosity is a constant. (If the viscosity $\nu = 0$, the slope vanishes, and the corresponding axis is horizontal.) The symmetry with respect to $z_t = 0$ is disturbed by the slope. Now we compare this slightly asymmetrical typical data curve with the symmetrical energy level curves, see Figure 9. Solutions of Eq. (8) with different initial values of $z(z_t = 0)$ give a set of energy level curves. The red curve is the data curve, the movement occurs in the direction ABCD. Energy is gained twice in each cycle (gait) in a phase of a "step", BC, and in a phase of a "fall" (in general not free fall), DA. The maximum of the energy occurs at

points A and C, the minimum occurs when at points B and D. There is a natural desire to find an approximation that considers the viscosity and the restoring force.

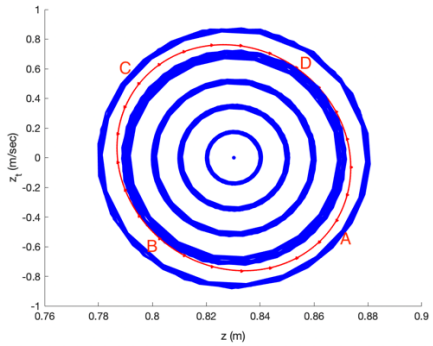

Fig 9. The energy level curves (blue) and the data curve (red) in the phase plane (z,z_t). The absolute value of the slope AC multiplied by mass m is the viscosity ν

7.2. A best fitting curve for a non homogeneous differential equation We identified the best fitting curve in the form

$$(12)\ z_{tt} + vz_t + kz_0^2(z - z_0) - k(z - z_0)^3 = fcos(\Omega t - \varphi),$$

where the term vz_t is the linear approximation of the damping force divided by mass. The constant $f = \frac{F}{m}$, where F is the amplitude of the excitation force, Ω is the angular frequency of the excitation force. The gravitation constant g is involved in the equation in a similar way as for the two already discussed models. As in the previous models, the equation for the best fitting curve was interpreted as a second order differential equation. The solution of the equation was computed and plotted in the same system of coordinates as the data curve. However, the balance between the viscosity and excitation force was too delicate, and most solution curves became stable spirals.

8. CONCLUSION

We introduced a new method for the investigation of human gait. This method is based on the visualisation of the vertical component of the movement of the COM during walking or running, in the space of the coordinates position, velocity, and acceleration of the centre of mass. We suggested a model by a non-linear homogeneous differential equation. We also had a partial success in approximation of the movement by a second order non-linear non-homogeneous differential equation. In this paper, we concentrated on features that are common for walking and for running. The individual features of the curves are of special interest for sport science, because they point to uncomfortableness in walking or running. We plan to investigate possible reasons for injuries by determining how stress is generated. One possible idea is to investigate why female runners have more frequent ACL (anterior cruciate ligament) tears than men [27].

ACKNOWLEGMENTS

The study followed ethical protocols as per ethics requirements (HE19- 239). Thanks to computer science students Ben Fisk, Danielle Galvin and Jarra McIntyre for developing a prototype of the software used for this paper and to sport science student Megan Bancks for the literature research. Thanks to Adam Harris and Gerd Schmalz for their critical comments and support.

References

1. Bullimore SR, Burn JF. Consequences of forward translation of the point of force application for the mechanics of running. Journal of Theoretical Biology. 2006;238:211–219.
2. Lipfert SW, Gunther M, Renjewski D, Grimmer S, Seyfarth A. A model-experiment comparison of system dynamics for human walking and running. Journal of Theoretical Biology. 2012;292:11–17.
3. Blickhan R. The spring-mass model for running and hopping. Journal of Biomechanics. 1989;22(11):1217–1227. doi:https://doi.org/10.1016/0021-9290(89)90224-8.
4. Blum Y, Lipfert SW, Seyfarth A. Effective leg stiffness in running. Journal of Biomechanics. 2009;42(14):2400–2405. doi:https://doi.org/10.1016/j.jbiomech.2009.06.040.
5. Ferris DP, Louie M, Farley CT. Running in the real world: adjusting leg stiffness for different surfaces. Proceedings of the Royal Society B: Biological Sciences. 1998;265(1400):989–994.
6. Nikooyan AA, Zadpoor AA. Mass–spring–damper modelling of the human body to study running and hopping – an overview. Proceedings of the Institution of Mechanical Engineers, Part H: Journal of Engineering in Medicine. 2011;225(12):1121–1135. doi:10.1177/0954411911424210.
7. Silder A, Besier T, Delp SL. Running with a load increases leg stiffness. Journal of Biomechanics. 2015;48(6):1003–1008. doi:10.1016/j.jbiomech.2015.01.051.
8. Bullimore SR, Burn JF. Ability of the planar spring–mass model to predict mechanical parameters in running humans. Journal of Theoretical Biology. 2007;248(4):686–695. doi:https://doi.org/10.1016/j.jtbi.2007.06.004.
9. Farley CT, Gonza´lez O. Leg stiffness and stride frequency in human running. Journal of Biomechanics. 1996;29(2):181–186. doi:https://doi.org/10.1016/0021-9290(95)00029-1.
10. Dalleau G, Belli A, Bourdin M, Lacour JR. The spring-mass model and the energy cost of treadmill running. European Journal of Applied Physiology and Occupational Physiology. 1998;77(3):257–263. doi:10.1007/s004210050330.
11. . Kuo AD. Stabilization of Lateral Motion in Passive Dynamic Walking. The International Journal of Robotics Research. 1999;18((9)):917–930.
12. Donelan JM, Kram R, Kuo AD. Simultaneous positive and negative external and mechanical work in human walking. Journal of Biomechanics. 2002;35:117–124.
13. Mochon S, McMahon TA. Ballistic Walking. Journal of Biomechanics. 1980;13(1):49–57.
14. Geyer H, Seyfarth A, Blickhan R. Compliant leg behaviour explains basic dynamics of walking and running. Proc Biol Sci. 2006;273(1603):2861-2867. doi:10.1098/rspb.2006.3637. Proc Biol Sci. 2006;273(1603):2861–2867.
15. Hong H, Kim S, Kim C, Lee S, Park S. Spring-like gait mechanics observed during walking in both young and older adults. Journal of Biomechanics. 2013;46:77–82.
16. Jung CK, Park S. Compliant bipedal model with the centre of pressure excursion associated with the oscillatory behaviour of the centre of mass reproduces the human gait dynamics. Journal of Biomechanics. 2014;47(223-229).
17. Kim S, Park S. Leg stiffness increased with speed to modulate gait frequency and propulsion energy. Journal of Biomechanics. 2011;44:1253–1258.
18. Song H, Park H, Park S. A springy pendulum could describe the swing leg kinetics of human walking. Journal of Biomechanics. 2016;49:1504–1509.
19. Ludwig C, Grimmer S, Seyfarth A, Maus HM. Multiple-step model-experiment matching allows precise definition of dynamical leg parameters in human running. Journal of Biomechanics. 2012;45:2472–2475.
20. Maus HM, Revzen S, Guckenheimer J, Ludwig C, Reger J, Seyfarth A. Constructing predictive models of human running. J R Soc Interface. 2015;12.
21. Fukuchi CA, Fukuchi RK, Duarte M. A public dataset of running biomechanics and the effects of running speed on lower extremity kinematics and kinetics. PeerJ. 2017;5(e3298).
22. Fukuchi CA, Fukuchi RK, Duarte M. A public dataset of overground and treadmill walking kinematics and kinetics in healthy individuals. PeerJ. 2018;6(e4640).
23. Hook R. Micrographia: or, Some Physiological Descriptions of Minute Bodies Made by Magnifying Glasses, With Observations and Inquiries Thereupon. London: Printed by J. Martyn and J. Allestry; 1665.
24. Hausdorff JM. Gait dynamics, fractals and falls: finding meaning in the stride-to-stride fluctuations of human walking. Human Movement Science. 2007;26:555–589.
25. Jordan D, Smith P. Nonlinear Ordinary Differential Equations. fourth edition ed. Oxford University Press; 2007.
26. Brennan MJ, Kovacic I. The Duffing Equation: Nonlinear Oscillators and their Behaviour. John Wiley and Sons; 2011.
27. Stefani R. Kinesiology Analysis of Athletics at the Ancient Olympics and of Performance Differences Between Male and Female Olympic Champions at the Modern Games in Running, Swimming and Rowing. Athens Journal of Sports. 2017;4(2):123–138.